Received: 24 April 2022 | Revised: 10 July 2022 | Accepted: 21 July 2022

DOI: 10.1002/dmrr.3570

RESEARCH ARTICLE

WILEY

A novel model for detecting advanced fibrosis in patients with nonalcoholic fatty liver disease

Xinyu Yang[1,2] | Mingfeng Xia[1,2] | Xinxia Chang[1,2] | Xiaopeng Zhu[1,2] | Xiaoyang Sun[1,2] | Yinqiu Yang[1,2] | Liu Wang[1,2,3] | Qiling Liu[1,2] | Yuying Zhang[1,2] | Yanlan Xu[1,2,4] | Huandong Lin[1,2] | Lin Liu[1,2] | Xiuzhong Yao[5] | Xiqi Hu[6] | Jian Gao[7] | Hongmei Yan[1,2] | Xin Gao[1,2] | Hua Bian[1,2,8]

[1]Department of Endocrinology and Metabolism, Zhongshan Hospital, Fudan University, Shanghai, China

[2]Fudan Institute for Metabolic Disease, Fudan University, Shanghai, China

[3]Second Affiliated Hospital of Army Military Medical University, Chongqing, China

[4]Department of Geriatrics, Qingpu Branch of Zhongshan Hospital, Fudan University, Shanghai, China

[5]Department of Radiology, Zhongshan Hospital, Fudan University, Shanghai, China

[6]Department of Pathology, Shanghai Medical College, Fudan University, Shanghai, China

[7]Department of Clinical Nutrition, Zhongshan Hospital, Center of Clinical Epidemiology, EBM of Fudan University, Fudan University, Shanghai, China

[8]Department of Endocrinology and Metabolism, Wusong Branch of Zhongshan Hospital, Fudan University, Shanghai, China

Correspondence
Hua Bian, Xin Gao and Hongmei Yan, Department of Endocrinology and Metabolism, Zhongshan Hospital, Fudan University, Fudan Institute for Metabolic Disease, Fudan University, 180 Fenglin Road, Shanghai 200032, China.
Email: zhongshan_bh@126.com, zhongshan_endo@126.com and yan.hongmei@zs-hospital.sh.cn

Funding information
Science and Technology Commission of Shanghai Municipality, Grant/Award Number: 20ZR1410200; Clinical Research Project of Zhongshan Hospital, Grant/Award Number: 2020ZSLC19; Shanghai Municipal Population and Family Planning Commission, Grant/Award Number: 201740092; Special Project of Integrating Traditional Chinese and Western Medicine in Shanghai General Hospital from the Shanghai Municipal Population and Family Planning Commission and Shanghai TCM Development Office,

Abstract

Aims: The study aimed to develop a novel noninvasive model to detect advanced fibrosis based on routinely available clinical and laboratory tests.

Materials and Methods: A total of 309 patients who underwent liver biopsy were randomly divided into the estimation group ($n = 201$) and validation group ($n = 108$). The model was developed using multiple regression analysis in the estimation group and further verified in the validation group. Diagnostic accuracy was evaluated using the receiver operating characteristic (ROC) curve.

Results: The model was named NAFLD Fibrosis Index (NFI): $-10.844 + 0.046 \times$ age $- 0.01 \times$ platelet count $+ 0.19 \times$ 2h postprandial plasma glucose (PG) $+ 0.294 \times$ conjugated bilirubin $- 0.015 \times$ ALT $+ 0.039 \times$ AST $+ 0.109 \times$ total iron binding capacity $-0.033 \times$ parathyroid hormone (PTH). The area under the ROC curve (AUC) of NFI was 0.86 (95% CI: 0.79–0.93, $p < 0.001$) in the estimation group and 0.80 (95% CI: 0.69–0.91, $p < 0.001$) in the validation group, higher than NFS, FIB4, APRI, and BARD, and similar to FibroScan (NFI AUC = 0.77, 95% CI: 0.66–0.89, $p = 0.001$ vs. FibroScan AUC = 0.76, 95% CI: 0.62–0.90, $p = 0.002$). By applying the low cut-off

Abbreviations: 2h PG, 2h postprandial plasma glucose; ALT, alanine aminotransferase; AST, aspartate aminotransferase; AUC, area under the ROC curve; NAFLD, nonalcoholic fatty liver disease; NASH, nonalcoholic steatohepatitis; NFI, NAFLD Fibrosis Index; NPV, negative predictive value; PPV, positive predictive value.; PTH, parathyroid hormone; ROC curve, receiver operating characteristic curve; T2DM, type 2 diabetes.

Xinyu Yang, Mingfeng Xia and Xinxia Chang have contributed equally to this work and share first authorship

Grant/Award Number: ZY(2018-2020)-FWTX-3019

value (−2.756), advanced fibrosis could be excluded among 49.3% and 48% of patients in the estimation group (sensitivity: 93.1%, NPV: 97.9%, specificity: 55.2%, and PPV: 26.0%) and validation group (sensitivity: 81.3%, NPV: 94.2%, specificity: 53.3%, and PPV: 23.2%), respectively, allowing them to avoid liver biopsy.

Conclusions: The study has established a novel model for advanced fibrosis, the diagnostic accuracy of which is superior to the current clinical scoring systems and is similar to FibroScan.

KEYWORDS
advanced fibrosis, diagnosis, logistic models, nonalcoholic fatty liver disease

1 | INTRODUCTION

Nonalcoholic fatty liver disease (NAFLD), the hepatic manifestation of metabolic syndrome that is frequently co-existing with obesity, type 2 diabetes (T2DM), and insulin resistance, has become one of the most common causes leading to chronic liver injury and affected approximately 25% of people worldwide.[1,2] The disease has a spectrum of histologic features ranging from steatosis without fibrosis to nonalcoholic steatohepatitis (NASH) with varying stages of fibrosis.[3] Advanced fibrosis (fibrosis stage ≥3) has been strongly implicated with long-term risk of the adverse outcomes such as cellular carcinoma and hepatic decompensation, which is one of the main causes of liver transplantation.[4–6] Meanwhile, advanced fibrosis increased the risks of extrahepatic metabolic disorders and complications.[7,8] As a consequence, patients with NAFLD should be assessed for the extent of fibrosis, especially the presence of advanced fibrosis, to optimise their management.

Up to now, liver biopsy is still the gold standard for evaluating fibrosis, but it is not recommended for routine screening and follow-up monitoring because of its invasive nature and high cost.[9,10] Noninvasive diagnosis is particularly important.[11,12] Elastography, the most common ones being FibroScan and MRE, is based on the measurement of vibration-induced shear waves through liver tissue,[13] but its application is limited by equipment conditions and the requirement of specialised technicians.[14,15] Nowadays, a number of noninvasive scoring systems such as NAFLD fibrosis score (NFS), Fibrosis-4 index (FIB-4), aspartate aminotransferase to platelet ratio index (APRI) and BARD have been applied to evaluate the progression of hepatic fibrosis, all of which can be calculated through clinical features and routine biochemical tests that are easily accessible. However, the diagnostic performances of these models were insufficiently accurate, and most of them were developed in patients with chronic liver diseases, such as viral hepatitis.[16–18] In the last decade, many patented biomarkers have also emerged, including PRO-C3, a commercially available assay for collagen type III synthesis, as well as algorithm models FibroTest® and ELF™.[19–21] Despite their improved diagnostic performance, the wide applications have been limited due to high costs and poor availability of patented biomarker tests. In addition, some other approaches exploring fibrosis markers including proteomics, metabolomics, and MicroRNA are in the experimental stage. Therefore, there is still an urgent need for a convenient and accurate noninvasive approach for advanced fibrosis.

The study aims to establish a novel model based on routine blood tests for advanced fibrosis, with more accurate diagnostic performance, providing clinical advice for noninvasive diagnosis of advanced fibrosis among NAFLD patients.

2 | METHODS

2.1 | Patients

A total of 309 patients with NAFLD who underwent liver biopsy in Zhongshan Hospital between 2011 and 2020 were recruited, 87 of whom received FibroScan examination at the same time. Exclusion criteria were as follows: (1) patients with a history of excessive alcohol consumption (>30 g/day for a man and >20 g/day for a woman) and (2) evidence of other liver damage such as viral or autoimmune hepatitis, drug-induced fatty liver, or Wilson's disease. All subjects were randomly divided into two groups in a ratio of 2:1 according to random numbers, the estimation group (n = 201) and the validation group (n = 108). The random numbers were generated via SPSS. The FibroScan group consisted of patients who simultaneously received FibroScan examination among all liver biopsy subjects. The medical history, physical characteristics, and serological examination of each patient were recorded during admission. The whole process conformed to the ethical guidelines of the Declaration of Helsinki and was approved by the local Ethics Committees (B2021-620). All patients gave written informed consent before being included in this study.

2.2 | Liver biopsy

Under the guidance of ultrasound, percutaneous liver biopsy was performed for each patient using 16G-needle from the right lobe of

liver. Pathological examinations were analysed by the same senior expert specialised in hepatology and blinded to other patient data. Liver fibrosis was evaluated in accordance to the NASH Clinical Research Network scoring system. Fibrosis was divided into stage 0–4. Stage 0: no fibrosis; stage 1: perisinusoidal or portal/periportal fibrosis; stage 2: perisinusoidal and portal/periportal fibrosis; stage 3: bridging fibrosis; and stage 4: cirrhosis. Advanced fibrosis was defined as fibrosis stage ≥3.

2.3 | Physical and serological examination

All patients received physical and serological examinations after admission. Height and weight were measured in the case of not wearing shoes. Body mass index (BMI) = weight (kg)/height $(m)^2$. Blood samples were collected locally after fasting for at least 12 h and then shipped to the clinical laboratory of Zhongshan hospital. The Hitachi 7600 automatic modern biological analyser was used to detect the total cholesterol (TC), triglyceride (TG), high-density-lipoprotein cholesterol (HDL-c), low-density-lipoprotein cholesterol (LDL-c), albumin, alanine aminotransferase (ALT), and aspartate aminotransferase (AST). TG and TC were determined using the oxidase method, and the rate method was used to determine the level of transaminase. Fasting plasma glucose (FPG) and 2h postprandial plasma glucose (PG) were measured using the glucose oxidase method, and haemoglobin A_{1c} (HbA_{1c}) was measured using high performance liquid chromatography. Parathyroid hormone (PTH) was determined using electrogenerated chemiluminescence.

2.4 | Noninvasive clinical scoring systems

The following clinical scoring systems were calculated according to published formulas and then compared with this novel model: NFS, FIB-4, APRI, and the BARD score.

2.5 | FibroScan examination

Liver stiffness measurement was performed using the M probe of FibroScan. The patient was lying flat on his/her back after having fasted for 2 h, with the right arm tucked behind the head. The medical ultrasound couplant was applied to the tip of the probe and the probe was placed on the skin between the rib bones at the level of the right lobe of the liver. With the assistance of ultrasound images, an area of at least 6 cm thick without large blood vessel structures was selected. The entire procedure lasts no more than 5 min. The examinations of all patients were performed by the same operator blinded to liver biopsy results. Acquisitions that do not have the correct vibration shape or correctly track the vibration propagation would be automatically rejected by the software. Ten valid measurements were obtained from each patient and the ratio of the successful measurement times over the total times (success rate) was calculated. The result was considered reliable only when the success rate was ≥60% and the interquartile range/median was ≤30%. The median value was kept as a representative result. Liver stiffness measurement results are expressed in kilopascals (kPa).

2.6 | Statistical analysis

The analysis of variance was used for comparison between multiple groups with normal distribution and homogeneity of variance. The Kruskal–Wallis test was used for variables without normal distribution or homogeneity of variance. The R × C chi-square test was used for categorical variables. The pathological presence or absence of advanced fibrosis was set as the dependent variable. The interaction and collinearity between variables have been first tested. Prior to modelling, the linearity test was performed on each quantitative variable to ensure all of them were linearly associated with the dependent variable. The interaction and collinearity have been tested and there was no collinearity between variables. Variables with $p < 0.2$ in the estimation group through univariate analysis were included in the multiple backward stepwise logistic regression analysis to determine the independent correlated variables for advanced fibrosis and establish a noninvasive diagnostic model. The Hosmer–Lemeshow goodness of fit test with a calibration curve was used to evaluate the calibration of the model, and the receiver operating characteristic (ROC) curve was used to evaluate the discrimination. A cut-off value with sensitivity or specificity ≥90% was determined for exclusion and diagnosis, respectively. The model derived from the estimation group was then applied to the validation group to test the diagnostic accuracy. Comparison of the diagnostic accuracy of the model with clinical scoring systems and FibroScan were conducted using the ROC curve. All statistical analyses were carried out using SPSS 23.0. ROC curves were conducted using MedCalc 20.0 and GraphPad 8.

3 | RESULTS

3.1 | Basic characteristics of patient population

The basic characteristics of 309 patients were detailed in Table 1. About half was male. The estimation group included 201 patients, validation group included 108 patients, and FibroScan group included 87 patients. Mean age of estimation, validation, and FibroScan group was 45.7 ± 14.8, 43.3 ± 14.9, and 42.9 ± 14.6 years, respectively. Mean BMI was 27.6 ± 4.7, 29.0 ± 4.3, and 29.1 ± 4.4 kg/m^2, respectively. No significant difference was found in FPG, 2h PG, HbA_{1c}, duration of diabetes, ALT, AST, AST/ALT, TG, TC, LDL-c, HDL-c, creatinine, uric acid, 25-(OH)-D, PTH, ferritin, total iron binding capacity, total bilirubin, and conjugated bilirubin between groups. Among the total patients, 78 cases (25.2%) had no pathological fibrosis, while 45 cases (14.6%) had advanced fibrosis. There was no significant difference between the estimation and validation group.

TABLE 1 Basic characteristics of the patient population

	Estimation group	Validation group	FibroScan group	*p* value
Total, *n*	201	108	87	
Sex, male/female	105/96	54/54	45/42	0.923
Age, year	45.7 ± 14.8	43.3 ± 14.9	42.9 ± 14.6*	0.301
BMI, kg/m^2	27.6 ± 4.7	29.0 ± 4.3	29.1 ± 4.4*	0.024
FPG, mmol/L	6.1 ± 2.0	5.9 ± 1.6	6.0 ± 1.7	0.343
2h PG, mmol/L	11.6 ± 4.5	11.3 ± 4.1	11.6 ± 4.0	0.800
HbA1c, %	6.9 ± 1.8	6.8 ± 1.8	6.9 ± 1.9	0.989
Duration of diabetes, y	0 (0, 1)	0 (0, 2)	0 (0, 2)	0.141
Platelet count, 10^9/L	219.2 ± 52.4	235.1 ± 58.7*	234.2 ± 60.4**	0.002
Albumin, g/L	43.5 ± 5.0	45.0 ± 4.5**	44.9 ± 4.5**	<0.001
ALT, U/L	61 (24, 98)	56 (39, 93)	67 (39, 89)	0.345
AST, U/L	35 (21, 57)	35 (27, 49)	36 (26, 50)	0.549
AST/ALT	0.63 (0.50, 0.89)	0.62 (0.47, 0.78)	0.62 (0.48, 0.77)	0.103
Triglycerides, mmol/L	1.8 (1.2, 2.5)	1.9 (1.2, 2.7)	1.9 (1.2, 2.6)	0.868
Total cholesterol, mmol/L	4.7 ± 1.2	4.6 ± 1.2	4.6 ± 1.2	0.348
LDL cholesterol, mmol/L	2.6 (2.0, 3.1)	2.6 (1.9, 3.1)	2.6 (2.0, 3.0)	0.886
HDL cholesterol, mmol/L	1.1 ± 0.4	1.0 ± 0.3	1.0 ± 0.3	0.494
Total bilirubin, umol/L	10.0 (7.9, 12.9)	11.0 (8.5, 13.6)	11.0 (8.5, 13.6)	0.270
Conjugated bilirubin, umol/L	3.6 (2.8, 4.6)	3.3 (2.6, 4.5)	3.3 (2.6, 4.4)	0.471
Creatinine, μmol/L	66 (54, 78)	69 (59, 82)	68 (56, 79)	0.628
Uric acid, μmol/L	364.2 ± 96.7	389.8 ± 95.6	383.7 ± 98.3	0.027
25-(OH)-D, nmol/L	40.5 ± 16.3	40.9 ± 16.3	39.3 ± 15.8	0.818
PTH, pg/mL	43.9 ± 16.1	41.9 ± 16.2	42.8 ± 17.1	0.563
Ferritin, ng/mL	310 (175, 520)	344 (197, 492)	342 (200, 494)	0.957
Total iron binding force, μmol/L	52.9 ± 7.5	54.8 ± 8.2	54.9 ± 8.7	0.071
Fibrosis stage, *n* (%)				
0	65 (32.3)	13 (12.0)	5 (5.7)	
1	57 (28.4)	40 (37.0)	36 (41.4)	
2	50 (24.9)	39 (36.1)	32 (36.8)	
3	22 (10.9)	13 (12.0)	11 (12.6)	
4	7 (3.5)	3 (2.8)	3 (3.4)	

Note: All data are expressed as the mean ± SD, medians (interquartile range), or *n* (%), as appropriate.

Abbreviations: 2h PG, 2h postprandial plasma glucose; ALT, alanine aminotransferase; AST, aspartate aminotransferase; BMI, body mass index; FPG, fasting plasma glucose; HbA1c, haemoglobin A1c; PTH, parathyroid hormone.

*$p < 0.05$ versus Estimation Group; **$p < 0.01$ versus Estimation Group.

3.2 | Candidate variables selection

In the estimation group, variables with $p < 0.2$ using univariate logistic analyses were selected as candidate variables, including sex, age, BMI, fasting plasma glucose (FPG), 2h postprandial plasma glucose (PG), HbA1c, duration of diabetes, platelet count, ALT, AST, AST/ALT, conjugated bilirubin, creatinine, uric acid, ferritin, and total iron binding capacity. It is worth noting that parathyroid hormone (PTH) was significantly associated with advanced fibrosis in the validation group (Table 2). In addition, some previous studies have pointed out the relationship between PTH and fibrosis.[22,23] Therefore, PTH was also identified as a candidate variable for model building.

TABLE 2 Univariate logistic regression of advanced fibrosis

	Estimation group (n = 201)		Validation group (n = 108)	
	OR (95% CI)	p value	OR (95% CI)	p value
Sex, male/female	1.776 (0.939–3.360)	0.077	1.759 (0.715–4.328)	0.219
Age, year	1.028 (1.006–1.051)	0.013	1.028 (0.997–1.061)	0.077
BMI, kg/m^2	1.061 (0.994–1.134)	0.076	1.038 (0.939–1.147)	0.469
FPG, mmol/L	1.177 (1.025–1.352)	0.021	1.213 (0.952–1.545)	0.118
2h PG, mmol/L	1.165 (1.083–1.253)	<0.001	1.244 (1.098–1.410)	0.001
HbA1c, %	1.289 (1.093–1.521)	0.003	1.353 (1.077–1.699)	0.009
Duration of diabetes, y	1.124 (1.041–1.215)	0.003	1.245 (1.116–1.390)	<0.001
Platelet count, 10^9/L	0.992 (0.986–0.999)	0.018	0.991 (0.983–1.000)	0.046
Albumin, g/L	0.997 (0.932–1.068)	0.941	0.902 (0.794–1.025)	0.113
ALT, U/L	1.009 (1.004–1.014)	<0.001	1.001 (0.992–1.010)	0.841
AST, U/L	1.022 (1.011–1.033)	<0.001	1.009 (0.993–1.026)	0.261
AST/ALT	0.486 (0.182–1.303)	0.152	1.072 (0.253–4.546)	0.925
Triglycerides, mmol/L	0.911 (0.751–1.106)	0.348	0.892 (0.679–1.172)	0.411
Total cholesterol, mmol/L	0.848 (0.631–1.140)	0.275	0.790 (0.506–1.233)	0.299
LDL cholesterol, mmol/L	0.907 (0.638–1.290)	0.587	0.759 (0.439–1.312)	0.323
HDL cholesterol, mmol/L	1.055 (0.443–2.512)	0.904	0.726 (0.172–3.058)	0.662
Total bilirubin, umol/L	1.032 (0.977–1.090)	0.262	0.994 (0.908–1.088)	0.890
Conjugated bilirubin, umol/L	1.181 (1.031–1.353)	0.016	0.880 (0.666–1.162)	0.367
Creatinine, μmol/L	0.974 (0.953–0.995)	0.018	0.969 (0.939–1.000)	0.053
Uric acid, μmol/L	0.997 (0.994–1.000)	0.075	0.994 (0.989–0.999)	0.031
25-(OH)-D, nmol/L	0.995 (0.975–1.015)	0.626	1.025 (0.996–1.054)	0.093
PTH, pg/mL	0.989 (0.968–1.011)	0.326	0.935 (0.892–980)	0.005
Ferritin, ng/mL	1.001 (1.000–1.002)	0.086	1.000 (0.998–1.002)	0.848
Total iron binding force, μmol/L	1.058 (1.009–1.109)	0.019	1.032 (0.976–1.091)	0.272

Abbreviations: 2h PG, 2h postprandial plasma glucose; ALT, alanine aminotransferase; AST, aspartate aminotransferase; BMI, body mass index; CI, confidence interval; FPG, fasting plasma glucose; HbA1c, haemoglobin A1c; PTH, parathyroid hormone.

3.3 | Model building

Incorporating the above 17 candidate variables into multiple logistic regression to construct the model, we finally identified eight variables independently associated with advanced fibrosis: age, platelet, 2h PG, conjugated bilirubin, ALT, AST, total iron binding capacity, and PTH (Table 3). There was a tendency for platelet count, ALT, and PTH to be excluded as p value is slightly larger than 0.05, but the diagnostic accuracy was higher when they were kept in the model. On this basis, we decided to retain these three variables and constructed a novel model named NAFLD fibrosis index (NFI). The formula is as follows: NFI = −10.844 + 0.046 × age − 0.01 × platelet count + 0.19 × 2h PG + 0.294 × conjugated bilirubin − 0.015 × ALT + 0.039 × AST + 0.109 × total iron binding capacity − 0.033 × PTH (Hosmer–Lemeshow χ^2 = 6.936, p = 0.544 > 0.05, Nagelkerke's R^2 = 0.392). The model had an area under the ROC curve (AUC) of 0.86 (95% CI: 0.79–0.93, $p < 0.001$), which was significantly superior to the common clinical scoring systems, including NFS, FIB-4, APRI, and BARD ($p < 0.001$ or $p < 0.01$). Furthermore, the calibration curve showed a robust calibration of the model (Figure 1, Table S1).

Using the ROC curve, the optimised cut-off value (−1.612) was identified based on the Youden index, with a sensitivity of 82.8% (95% CI: 64.2%–94.2%) and specificity of 82.0% (95% CI: 75.4%–87.4%). Besides, the cut-off value of sensitivity ≥90% (<−2.756) or specificity ≥90% (>−1.103) was determined for exclusion and diagnosis of advanced fibrosis (Figure 2). By applying the low cut-off value (<−2.756), 97 (55.2%) of 174 patients without advanced fibrosis were correctly identified. Among patients without advanced fibrosis, only two were incorrectly staged, with a high negative predictive value (NPV) of 97.9% (95% CI: 92.5%–99.5%), superior to NFS, FIB-4, APRI, and BARD (Table S2, Table 4). Overall, the model identified the absence of advanced fibrosis in 49.3% [(97 + 2)/201] of

TABLE 3 Multivariate logistic regression of advanced fibrosis

	B	Standard error	Odds ratio (95% CI)	p value
Age, year	0.046	0.020	1.048 (1.006–1.090)	0.023
Platelet count, 10^9/L	−0.010	0.005	0.990 (0.980–1.000)	0.057
2h PG, mmol/L	0.190	0.064	1.209 (1.066–1.371)	0.003
Conjugated bilirubin, umol/L	0.294	0.108	1.342 (1.086–1.657)	0.006
ALT, U/L	−0.015	0.008	0.986 (0.970–1.001)	0.066
AST, U/L	0.039	0.015	1.040 (1.010–1.070)	0.008
Total iron binding force, μmol/L	0.109	0.038	1.115 (1.034–1.202)	0.005
PTH, pg/mL	−0.033	0.019	0.967 (0.932–1.003)	0.074
Constant	−10.844			<0.001

Abbreviations: 2h PG, 2h postprandial plasma glucose; ALT, alanine aminotransferase; AST, aspartate aminotransferase; CI, confidence interval; PTH, parathyroid hormone.

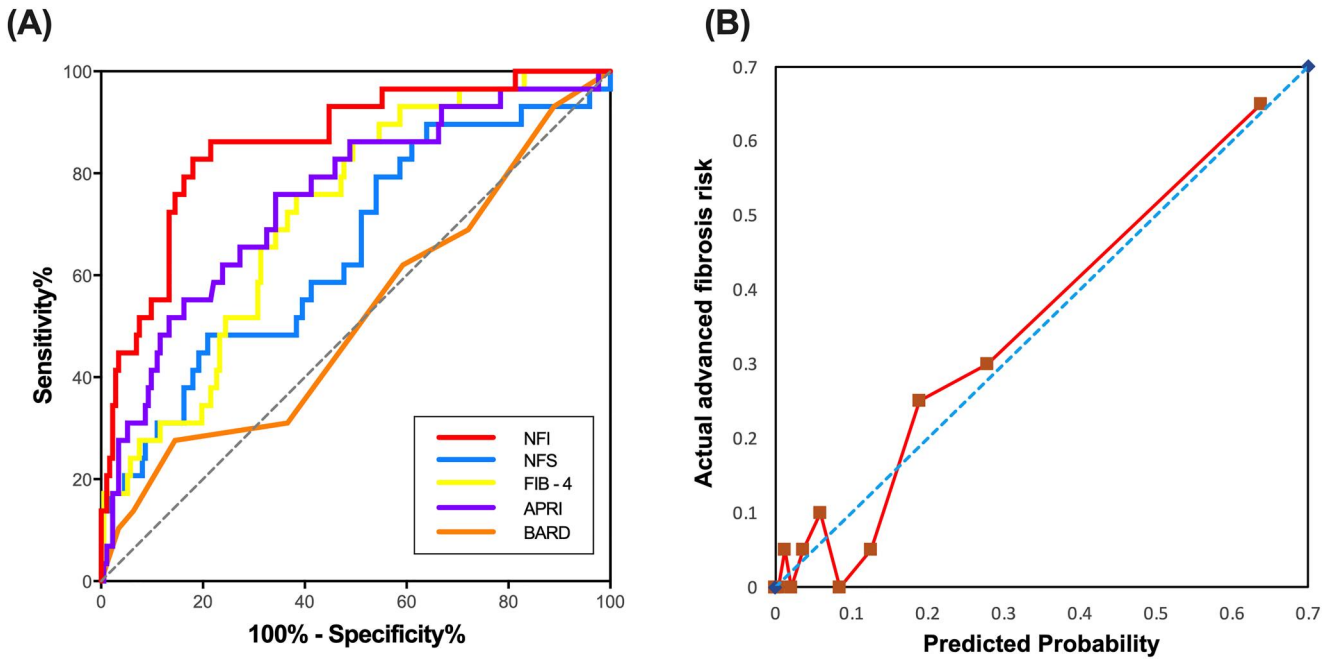

FIGURE 1 (A) The receiver operating characteristic curves of NFI and other clinical scoring systems for differentiating Stage 0–2 versus Stage 3–4 in the estimation group (n = 201). (B) Calibration curve for NFI in the estimation group. NFI, NAFLD Fibrosis Index

patients with a correct rate of 97.9% so that liver biopsy only needs to be performed in the remaining 50.7% of patients. The high cut-off value (>−1.103) correctly detected 16 (55.2%) out of 29 patients with advanced fibrosis, with a specificity of 90.1% (95% CI: 84.6%–94.1%). It is notable that NPV for a high cut-off value was still more than 90% (Table S2, Table 4).

3.4 | Validation of results

Next, the accuracy of NFI in distinguishing the presence or absence of advanced fibrosis was validated in 108 patients. The AUC remained high in the validation group, which reached up to 0.80 (95% CI: 0.69–0.91, p < 0.001). Although no significant statistical difference was found, the AUC of the new model was still higher than that of the other clinical scoring systems. Robust model calibration still remained in the validation group (Figure 3, Table S1). Further validation was carried out in the population that underwent FibroScan examination. The diagnostic accuracy of NFI was similar to that of FibroScan, and the AUC of NFI was 0.77 (95% CI: 0.66–0.89, p = 0.001) and the AUC of FibroScan was 0.76 (95% CI: 0.62–0.90, p = 0.002) (Figure 3B). In addition, the three cut-off values were also validated in validation group. The sensitivity and specificity of the optimised cut-off value (−1.612) was 68.8% (95% CI: 41.5%–87.9%) and 81.5% (95% CI: 71.8%–88.6%) in the validation group. The sensitivity of the low cut-off value (<−2.756) was 81.3% (95% CI: 53.7%–95.0%), which was slightly lower than that in the estimation group. 49 (53.3%) of the 92 patients without advanced fibrosis were

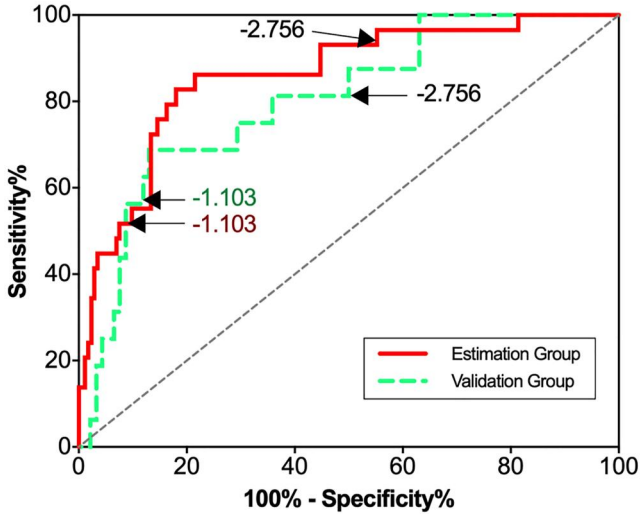

FIGURE 2 ROC curves of the NAFLD Fibrosis Index in the estimation group ($n = 201$) and validation group ($n = 108$). The area under the ROC curve for the estimation and validation groups was 0.86 (95% CI: 0.79–0.93, $p < 0.001$) and 0.80 (95% CI: 0.69–0.91, $p < 0.001$), respectively. The cut-off values with sensitivity ≥90% (< −2.756) and specificity ≥90% (>−1.103) have been marked with solid arrows on the ROC curves. ROC, receiver operating characteristic

correctly detected by the low cut-off value. By using this low cut-off value, the absence of advanced fibrosis could be identified with an NPV of 94.2% (95% CI: 83.1%–98.5%). The high cut-off value (> −1.103) still has a high degree of specificity (88.4%, 95% CI: 79.2%–93.6%) in the validation group. Among 16 patients, nine cases (56.3%) with advanced fibrosis were correctly detected. Similar to estimation group, the NPV also remained more than 90% in the validation group (Table S2, Table 4).

4 | DISCUSSION

In this study, we constructed a novel noninvasive model called NFI for advanced fibrosis. The model is composed of clinical and laboratory indicators that are routinely tested and easily accessible, with higher diagnostic accuracy for distinguishing the absence and presence of advanced fibrosis than clinical scoring systems including NFS, FIB-4, APRI, and BARD and with similar performance characteristics to FibroScan. There was a low and high cut-off value of NFI for advanced fibrosis exclusion and diagnosis, respectively. The NPV of the low cut-off value even reached up to 95%, which demonstrated that the model is an excellent tool for ruling out advanced fibrosis.

TABLE 4 Accuracy of the NFI for advanced fibrosis in the estimation and validation group

Group (*n*)	Model	Cut-off value	Se (%)	Sp (%)	PPV (%)	NPV (%)
Estimation group (201)	NFI	= −1.612	82.8 (64.2–94.2)	82.0 (75.4–87.4)	43.6 (35.1–52.6)	96.6 (92.7–98.4)
		<−2.756	93.1 (77.2–99.2)	55.2 (47.5–62.8)	26.0 (22.4–29.8)	97.9 (92.5–99.5)
		>−1.103	55.2 (35.7–73.6)	90.1 (84.6–94.1)	48.5 (35.0–62.2)	92.3 (88.8–94.7)
	NFS	<−1.45	72.4 (52.5–86.6)	46.5 (38.9–54.2)	18.6 (12.1–27.2)	90.9 (82.4–95.7)
		>0.67	17.2 (6.5–36.5)	97.1 (93.0–98.9)	50.0 (20.1–79.9)	87.4 (81.7–91.6)
	FIB-4	<1.30	51.7 (32.9–70.1)	69.8 (62.2–76.4)	77.6 (65.5–86.5)	89.6 (82.8–94.0)
		>3.25	13.8 (4.5–32.6)	99.4 (96.3–100.0)	80.0 (29.9–98.9)	87.2 (81.6–91.4)
	APRI	= 1	17.2 (6.5–36.5)	96.5 (92.2–98.6)	45.5 (18.1–75.4)	87.4 (81.6–91.6)
	BARD	= 2	31.0 (16.0–51.0)	63.4 (55.7–70.5)	12.5 (6.2–22.9)	84.5 (76.8–90.0)
Validation group (108)	NFI	= −1.612	68.8 (41.5–87.9)	81.5 (71.8–88.6)	39.3 (22.1–59.3)	93.8 (85.4–97.7)
		<−2.756	81.3 (53.7–95.0)	53.3 (42.6–63.6)	23.2 (13.4–36.7)	94.2 (83.1–98.5)
		>−1.103	56.3 (30.6–79.2)	88.4 (79.2–93.6)	45.0 (23.8–68.0)	90.0 (83.8–96.5)
	NFS	<−1.45	81.3 (53.7–95.0)	59.8 (49.0–69.7)	26.0 (15.1–40.6)	94.8 (84.7–98.7)
		>0.67	6.3 (0.3–32.3)	95.7 (88.6–98.6)	20.0 (1.1–70.1)	85.4 (76.8–91.4)
	FIB-4	<1.30	56.3 (30.6–79.2)	78.3 (68.2–85.9)	31.0 (16.0–51.0)	91.1 (82.0–96.1)
		>3.25	0 (0–24.1)	100.0 (95.0–100.0)	—	85.2 (76.8–91.0)
	APRI	= 1	0 (0–24.1)	97.8 (91.6–99.6)	0 (0–80.2)	84.9 (76.3–90.9)
	BARD	= 2	75.0 (47.4–91.7)	53.3 (42.6–63.6)	21.8 (12.2–35.4)	92.5 (80.9–97.6)

Abbreviations: NFI, NAFLD Fibrosis Index; NFS, NAFLD fibrosis score; NPV, negative predictive value; PPV, positive predictive value; Se, sensitivity; Sp, specificity.

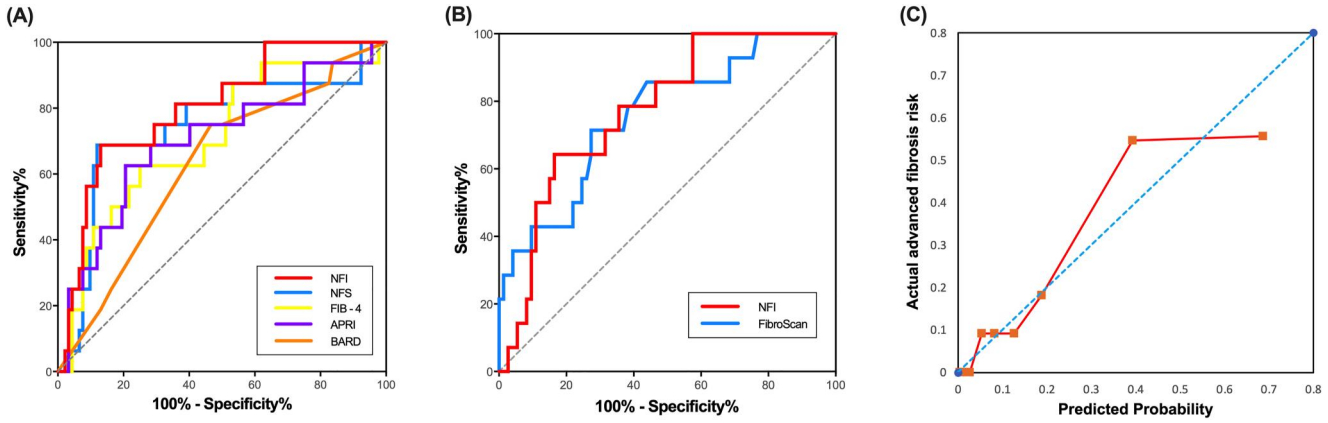

FIGURE 3 (A) ROC curves of NFI and other clinical scoring systems for differentiating Stage 0–2 versus Stage 3–4 in the validation group ($n = 108$). (B) ROC curves of NFI and FibroScan for differentiating Stage 0–2 versus Stage 3–4 among patients undergoing FibroScan examination ($n = 87$). (C) Calibration curve for NFI in the validation group. NFI, NAFLD Fibrosis Index; ROC, receiver operating characteristic

Early diagnosis of advanced fibrosis is crucial for the prognosis of NAFLD patients. 'Physical' imaging tests have high requirements on equipment institutions and specialised technicians, not suitable for resource-constrained environments. Serological tests, such as clinical scoring systems, are currently widely used in clinical practice, among which NFS and FIB-4 are the most accurate and can be used as first-line tools in primary care institutions.[18,24] However, these noninvasive approaches are either insufficiently accurate or have been derived from cohorts of patients with other chronic liver disease, such as HCV and HBV. As for patented tests, although biomarkers such as PRO-C3 combined with clinical indicators as well as Fibrometer® outperformed APRI, FIB-4, and NFS, the high cost and inconvenience of patented testing limit their wider application.[19,20] NAFLD fibrosis biomarkers through multi-omics and epigenetics are still in the experimental stage and are far from clinical application. There is still a lack of a simple and efficient noninvasive model for advanced fibrosis among NAFLD patients.

By using multiple logistics analysis, the study established a novel formula, which consists of eight common clinical indicators including age, platelet count, 2h PG, conjugated bilirubin, ALT, AST, total iron binding capacity, and PTH. The indicators can be easily obtained through medical history and blood tests. A number of previous studies have pointed out that age, platelet count, 2h PG, ALT, and AST are independently associated with advanced fibrosis.[16,25–27] When the course of the disease is unknown, age can reflect the duration of the disease to a certain extent.[25] It is known that the reduction of platelet count is associated with advanced fibrosis mainly due to hypersplenism caused by fibrosis.[26,27] As we know, ALT exists in the cytoplasm of the hepatocyte, and AST exists in the mitochondria of the hepatocyte. In the model, AST is positively associated with advanced fibrosis while ALT is negatively associated. This is because mitochondria are often involved when hepatocytes are severely damaged, and AST increases more significantly, especially in patients with advanced fibrosis.[28] Conjugated bilirubin is closely associated to hepatic lobular inflammation, and inflammation is the early stage of the fibrosis development process.[29] The Fibrometer® model proposed by Leroy et al. pointed out that ferritin was independently associated with advanced fibrosis, and another noninvasive scoring system also pointed out that ferritin was independently associated to NASH.[30] Iron loading has been frequently observed in chronic liver diseases in recent years. Excess iron may promote the Fenton reaction, produce a large number of radicals, cause serious cell and tissue damage, and lead to fibrosis.[31] Ferroptosis is a newly discovered form of cell death in recent years. Animal studies have shown that it affects the progression of nonalcoholic steatohepatitis by regulating lipid peroxidation-mediated cell death in mice.[30,32] On this basis, the study screened out a new indicator for advanced fibrosis related to iron load, that is, total iron binding capacity. It is noteworthy that PTH was significantly associated with advanced fibrosis when model building, and keeping it in the model significantly increased the AUC value. Several clinical literatures have pointed out the association between PTH and fibrosis, suggesting that PTH could be a predictor of the pathologic severity of NAFLD, but most of them were attributed to the disturbances of PTH-vitamin D axis in NAFLD and hepatic osteodystrophy.[22,23,33,34] However, there was no association between calcium, phosphorus, and vitamin D with fibrosis in this study, which implies that the association between PTH and fibrosis may be independent of calcium and phosphorus metabolism. Regrettably, the mechanism is still unclear and needs to be further explored.

Overall, the study successfully conducted a novel model for advanced fibrosis, with an AUC of more than 0.8, which reached an excellent level, and was similar to FibroScan. For primary health care institutions that cannot be equipped with FibroScan, it is a good alternative. These institutions once used NFS and FIB4 as primary screening tools. Compared with them, NFI was also based on routine blood and clinical test variables, but AUC was significantly superior to previous models such as NFS, FIB-4, APRI, and BARD, whose diagnostic accuracy were only acceptable levels in this study.[35] Improving diagnostic accuracy without increasing the clinical costs and ease of calculation (similar to NFS) raises the possibility of widespread

application. In addition, the low cut-off value of the model has an extremely high NPV of more than 90%, which is better than others. It indicated that the model was an excellent tool for ruling out advanced fibrosis. For large clinics, nearly half of NALFD patients with a low risk of fibrosis can be preliminarily excluded using this model, thereby reducing unnecessary liver biopsy.

However, this study still had several limitations. Firstly, the study is a cross-sectional study and lacks external validation. Longitudinal studies are necessary to further validate the effectiveness and stability of the current findings. Meanwhile, external validation in more and diverse populations is necessary prior to clinical application. Secondly, it is regrettable that PPV for diagnosis was not high enough, which is also a common problem of most noninvasive methods. As patients with NAFLD are generally less willing to undergo liver biopsy, samples were difficult to collect. From an ethical point of view, liver biopsy is not recommended for mild or severe patients, resulting in a small number of advanced fibrosis cases in the study. In the future, the sample size needs to be expanded, especially the number of positive cases, to improve the detection rate of the disease.

5 | CONCLUSION

The study proposed a noninvasive model for advanced fibrosis based on serological indicators. The diagnostic performance of this model is better than that of the common clinical scoring systems including NFS, FIB-4, APRI, BARD, and AST/ALT and is similar to FibroScan. Because of high NPV, the model is recommended for ruling out advanced fibrosis, which can reduce unnecessary liver biopsy to a certain extent.

AUTHOR CONTRIBUTIONS

Xinyu Yang: research design, statistical analyses and interpretation of the data, drafting, and revision of the manuscript; Mingfeng Xia: research design, statistics guidance and revision of the manuscript; Xinxia Chang: collection of the data, technical support; Xiaopeng Zhu and Xiaoyang Sun: collection of the data and assistance in data analysis; Yinqiu Yang, Liu Wang, Qiling Liu, Zhang Yuying, Yanlan Xu, Huandong Lin, and Lin Liu: collection of the data; Xiuzhong Yao and Xiqi Hu: imaging technical and histopathologic support; Jian Gao: statistical methods guidance; Hua Bian, Xin Gao and Hongmei Yan: research design and conduction, interpretation of the data, technical conduction, and critical revision of the manuscript. All authors have reviewed and approved to submit the final manuscript.

ACKNOWLEDGEMENTS

The authors gratefully acknowledge all the patients who participated in this study.

CONFLICT OF INTERESTS

The authors declare no conflicts of interest for the research conducted in this study.

DATA AVAILABILITY STATEMENT

The data that support the findings of this study are available from the corresponding author upon reasonable request.

ETHICS STATEMENT

The whole study process was approved by the Ethics Committees of Zhongshan Hospital (B2021-620), under the guidelines of the Declaration of Helsinki. All patients gave written informed consent before included in this study.

ORCID

Qiling Liu https://orcid.org/0000-0002-9412-5001
Hongmei Yan https://orcid.org/0000-0001-7341-4368
Xin Gao https://orcid.org/0000-0003-1864-7796
Hua Bian https://orcid.org/0000-0001-8449-0665

PEER REVIEW

The peer review history for this article is available at https://publons.com/publon/10.1002/dmrr.3570.

REFERENCES

1. Targher G, Corey KE, Byrne CD, Roden M. The complex link between NAFLD and type 2 diabetes mellitus – mechanisms and treatments. *Nat Rev Gastroenterol Hepatol*. 2021;18(9):599-612. https://doi.org/10.1038/s41575-021-00448-y
2. Younossi ZM. Non-alcoholic fatty liver disease – a global public health perspective. *J Hepatol*. 2019;70(3):531-544. https://doi.org/10.1016/j.jhep.2018.10.033
3. Powell EE, Wong VW, Rinella M. Non-alcoholic fatty liver disease. *Lancet*. 2021;397(10290):2212-2224. https://doi.org/10.1016/s0140-6736(20)32511-3
4. Pierantonelli I, Svegliati-Baroni G. Nonalcoholic fatty liver disease: basic pathogenetic mechanisms in the progression from NAFLD to NASH. *Transplantation*. 2019;103(1):e1-e13. https://doi.org/10.1097/tp.0000000000002480
5. Taylor RS, Taylor RJ, Bayliss S, et al. Association between fibrosis stage and outcomes of patients with nonalcoholic fatty liver disease: a systematic review and meta-analysis. *Gastroenterology*. 2020;158(6):1611-1625.e1612. https://doi.org/10.1053/j.gastro.2020.01.043
6. Hagström H, Nasr P, Ekstedt M, et al. Fibrosis stage but not NASH predicts mortality and time to development of severe liver disease in biopsy-proven NAFLD. *J Hepatol*. 2017;67(6):1265-1273. https://doi.org/10.1016/j.jhep.2017.07.027
7. Targher G, Tilg H, Byrne CD. Non-alcoholic fatty liver disease: a multisystem disease requiring a multidisciplinary and holistic approach. *Lancet Gastroenterol Hepatol*. 2021;6(7):578-588. https://doi.org/10.1016/s2468-1253(21)00020-0
8. Targher G, Byrne CD, Tilg H. NAFLD and increased risk of cardiovascular disease: clinical associations, pathophysiological mechanisms and pharmacological implications. *Gut*. 2020;69(9):1691-1705. https://doi.org/10.1136/gutjnl-2020-320622
9. Bedossa P, Dargère D, Paradis V. Sampling variability of liver fibrosis in chronic hepatitis C. *Hepatology*. 2003;38(6):1449-1457. https://doi.org/10.1053/jhep.2003.09022
10. Tapper EB, Lok AS. Use of liver imaging and biopsy in clinical practice. *N Engl J Med*. 2017;377(8):756-768. https://doi.org/10.1056/nejmra1610570
11. Castera L, Friedrich-Rust M, Loomba R. Noninvasive assessment of liver disease in patients with nonalcoholic fatty liver disease.

Gastroenterology. 2019;156(5):1264-1281.e1264. https://doi.org/10.1053/j.gastro.2018.12.036
12. Younossi ZM, Loomba R, Anstee QM, et al. Diagnostic modalities for nonalcoholic fatty liver disease, nonalcoholic steatohepatitis, and associated fibrosis. *Hepatology*. 2018;68(1):349-360. https://doi.org/10.1002/hep.29721
13. Selvaraj EA, Mózes FE, Jayaswal ANA, et al. Diagnostic accuracy of elastography and magnetic resonance imaging in patients with NAFLD: a systematic review and meta-analysis. *J Hepatol*. 2021;75:770-785.
14. Eddowes PJ, Sasso M, Allison M, et al. Accuracy of fibroscan controlled attenuation parameter and liver stiffness measurement in assessing steatosis and fibrosis in patients with nonalcoholic fatty liver disease. *Gastroenterology*. 2019;156(6):1717-1730. https://doi.org/10.1053/j.gastro.2019.01.042
15. Chalasani N, Younossi Z, Lavine JE, et al. The diagnosis and management of nonalcoholic fatty liver disease: practice guidance from the American Association for the Study of Liver Diseases. *Hepatology*. 2018;67(1):328-357. https://doi.org/10.1002/hep.29367
16. Lee J, Vali Y, Boursier J, et al. Prognostic accuracy of FIB-4, NAFLD fibrosis score and APRI for NAFLD-related events: a systematic review. *Liver Int*. 2021;41(2):261-270. https://doi.org/10.1111/liv.14669
17. Younes R, Caviglia GP, Govaere O, et al. Long-term outcomes and predictive ability of non-invasive scoring systems in patients with non-alcoholic fatty liver disease. *J Hepatol*. 2021;75(4):786-794. https://doi.org/10.1016/j.jhep.2021.05.008
18. Graupera I, Thiele M, Serra-Burriel M, et al. Low accuracy of FIB-4 and NAFLD fibrosis scores for screening for liver fibrosis in the population. *Clin Gastroenterol Hepatol*. 2021.
19. Daniels SJ, Leeming DJ, Eslam M, et al. ADAPT: an algorithm incorporating PRO-C3 accurately identifies patients with NAFLD and advanced fibrosis. *Hepatology*. 2019;69(3):1075-1086. https://doi.org/10.1002/hep.30163
20. Vali Y, Lee J, Boursier J, et al. FibroTest for evaluating fibrosis in non-alcoholic fatty liver disease patients: a systematic review and meta-analysis. *J Clin Med*. 2021:10.
21. Vali Y, Lee J, Boursier J, et al. Enhanced liver fibrosis test for the non-invasive diagnosis of fibrosis in patients with NAFLD: a systematic review and meta-analysis. *J Hepatol*. 2020;73(2):252-262. https://doi.org/10.1016/j.jhep.2020.03.036
22. Zhu X, Yan H, Chang X, et al. Association between non-alcoholic fatty liver disease-associated hepatic fibrosis and bone mineral density in postmenopausal women with type 2 diabetes or impaired glucose regulation. *BMJ Open Diabetes Res Care*. 2020;8(1):e000999. https://doi.org/10.1136/bmjdrc-2019-000999
23. Jamialahmadi T, Nematy M, Jangjoo A, et al. The predictive role of parathyroid hormone for non-alcoholic fatty liver disease based on invasive and non-invasive findings in candidates of bariatric surgery. *Eat Weight Disord*. 2021;27(2):693-700. https://doi.org/10.1007/s40519-021-01151-2
24. Schreiner AD, Zhang J, Durkalski-Mauldin V, et al. Advanced liver fibrosis and the metabolic syndrome in a primary care setting. *Diabetes Metab Res Rev*. 2021;37(8):e3452. https://doi.org/10.1002/dmrr.3452
25. Klisic A, Abenavoli L, Fagoonee S, Kavaric N, Kocic G, Ninić A. Older age and HDL-cholesterol as independent predictors of liver fibrosis assessed by BARD score. *Minerva Med*. 2019;110(3):191-198. https://doi.org/10.23736/s0026-4806.19.05978-0
26. Zhang H, Zhang S, Zhang J, et al. Improvement of human platelet aggregation post-splenectomy with paraesophagogastric devascularization in chronic hepatitis B patients with cirrhotic hypersplenism. *Platelets*. 2020;31(8):1019-1027. https://doi.org/10.1080/09537104.2019.1704715
27. Bucsics T, Lampichler K, Vierziger C, et al. Covered transjugular intrahepatic portosystemic shunt improves hypersplenism-associated cytopenia in cirrhosis. *Dig Dis Sci*. 2022. https://doi.org/10.1007/s10620-022-07443-6
28. Kamimoto Y, Horiuchi S, Tanase S, Morino Y. Plasma clearance of intravenously injected aspartate aminotransferase isozymes: evidence for preferential uptake by sinusoidal liver cells. *Hepatology*. 1985;5(3):367-375. https://doi.org/10.1002/hep.1840050305
29. Nguyen-Khac E, Thiele M, Voican C, et al. Non-invasive diagnosis of liver fibrosis in patients with alcohol-related liver disease by transient elastography: an individual patient data meta-analysis. *Lancet Gastroenterol Hepatol*. 2018;3(9):614-625. https://doi.org/10.1016/s2468-1253(18)30124-9
30. Tsurusaki S, Tsuchiya Y, Koumura T, et al. Hepatic ferroptosis plays an important role as the trigger for initiating inflammation in nonalcoholic steatohepatitis. *Cell Death Dis*. 2019;10(6):449. https://doi.org/10.1038/s41419-019-1678-y
31. Mehta KJ, Farnaud SJ, Sharp PA. Iron and liver fibrosis: mechanistic and clinical aspects. *World J Gastroenterol*. 2019;25(5):521-538. https://doi.org/10.3748/wjg.v25.i5.521
32. Qi J, Kim JW, Zhou Z, Lim CW, Kim B. Ferroptosis affects the progression of nonalcoholic steatohepatitis via the modulation of lipid peroxidation-mediated cell death in mice. *Am J Pathol*. 2020;190(1):68-81. https://doi.org/10.1016/j.ajpath.2019.09.011
33. Miroliaee A, Nasiri-Toosi M, Khalilzadeh O, Esteghamati A, Abdollahi A, Mazloumi M. Disturbances of parathyroid hormone-vitamin D axis in non-cholestatic chronic liver disease: a cross-sectional study. *Hepatol Int*. 2010;4(3):634-640. https://doi.org/10.1007/s12072-010-9194-2
34. Fisher L, Fisher A. Vitamin D and parathyroid hormone in outpatients with noncholestatic chronic liver disease. *Clin Gastroenterol Hepatol*. 2007;5(4):513-520. https://doi.org/10.1016/j.cgh.2006.10.015
35. Mandrekar JN. Receiver operating characteristic curve in diagnostic test assessment. *J Thorac Oncol*. 2010;5(9):1315-1316. https://doi.org/10.1097/jto.0b013e3181ec173d

SUPPORTING INFORMATION

Additional supporting information can be found online in the Supporting Information section at the end of this article.

How to cite this article: Yang X, Xia M, Chang X, et al. A novel model for detecting advanced fibrosis in patients with nonalcoholic fatty liver disease. *Diabetes Metab Res Rev*. 2022;38(8):e3570. https://doi.org/10.1002/dmrr.3570